Studies in Systems, Decision and Control 371

Muralindran Mariappan
Mohd Rizal Arshad
Rini Akmeliawati
Chong Shin Chong *Editors*

# Control Engineering in Robotics and Industrial Automation

## Malaysian Society for Automatic Control Engineers (MACE) Technical Series 2018

Springer

## Studies in Systems, Decision and Control

Volume 371

The series “Studies in Systems, Decision and Control” (SSDC) covers both new developments and advances, as well as the state of the art, in the various areas of broadly perceived systems, decision making and control–quickly, up to date and with a high quality. The intent is to cover the theory, applications, and perspectives on the state of the art and future developments relevant to systems, decision making, control, complex processes and related areas, as embedded in the fields of engineering, computer science, physics, economics, social and life sciences, as well as the paradigms and methodologies behind them. The series contains monographs, textbooks, lecture notes and edited volumes in systems, decision making and control spanning the areas of Cyber-Physical Systems, Autonomous Systems, Sensor Networks, Control Systems, Energy Systems, Automotive Systems, Biological Systems, Vehicular Networking and Connected Vehicles, Aerospace Systems, Automation, Manufacturing, Smart Grids, Nonlinear Systems, Power Systems, Robotics, Social Systems, Economic Systems and other. Of particular value to both the contributors and the readership are the short publication timeframe and the world-wide distribution and exposure which enable both a wide and rapid dissemination of research output.

Indexed by SCOPUS, DBLP, WTI Frankfurt eG, zbMATH, SCImago.

All books published in the series are submitted for consideration in Web of Science.

More information about this series at http://www.springer.com/series/13304

Muralindran Mariappan · Mohd Rizal Arshad ·
Rini Akmeliawati · Chong Shin Chong
Editors

# Control Engineering in Robotics and Industrial Automation

## Malaysian Society for Automatic Control Engineers (MACE) Technical Series 2018

Springer

*Editors*
Muralindran Mariappan
Faculty of Engineering
Universiti of Malaysia Sabah
Kota Kinabalu, Malaysia

Mohd Rizal Arshad
Faculty of Electrical Engineering Technology
Universiti Malaysia Perlis
Perlis, Malaysia

Rini Akmeliawati
School of Mechanical Engineering
The University of Adelaide
Adelaide, Australia

Chong Shin Chong
Faculty of Electrical Engineering
Universiti Teknikal Malaysia Melaka
Durian Tunggal, Malaysia

ISSN 2198-4182 ISSN 2198-4190 (electronic)
Studies in Systems, Decision and Control
ISBN 978-3-030-74539-4 ISBN 978-3-030-74540-0 (eBook)
https://doi.org/10.1007/978-3-030-74540-0



This Springer imprint is published by the registered company Springer Nature Switzerland AG
The registered company address is: Gewerbestrasse 11, 6330 Cham, Switzerland

# Preface

One of the main objectives of the Malaysian Society for Automatic Control Engineers (MACE) is to promote the science and technology of automatic control engineering in the broadest sense in all systems whether, for example, engineering, physical, biological, social, or economic, in both theory and application. For that, MACE organizes and sponsors technical meetings such as congresses, conferences, symposia, and workshops. And, this book is about the collection of all the technical series presented in the last 2 years.

Many books have been written on control engineering, describing new methods for controlling systems and better ways of mathematically formulating existing techniques to solve the ever-increasing complex problems faced by practicing engineers. However, few books fully address the application aspects of control engineering. It is the intention of this new series to redress this situation.

This series will stress application issues, and not just the mathematics of control engineering. It will provide texts that present not only both new and well-established techniques but also detailed examples of the applications of these methods to the solution of real-world problems. There are many exciting examples of the applications of control techniques in the established fields of electrical, mechanical, and biomedical engineering that discussed in this book. Among the applications, it includes the applications in the brake-by-wire system, assisted rehabilitation device for post-stroke patient, pollution monitoring and control, agriculture field, piano, virtual impact tests, underwater, and camera system.

This series presents books that draw on expertise from both the academic world and the applications domains and will be useful not only as academically recommended course texts but also as handbooks for practitioners in many applications domains. *Control Engineering in Robotics and Industrial Automation—Malaysian*

*Society for Automatic Control Engineers (MACE) Technical Series 2018* is another outstanding entry in Springer Technical Series.

Kota Kinabalu, Malaysia Muralindran Mariappan
Perlis, Malaysia Mohd Rizal Arshad
Adelaide, Australia Rini Akmeliawati
Durian Tunggal, Malaysia Chong Shin Chong

# Contents

# Notation for MACE Technical Series 2018

## Design and Control of a 3D Robot-Assisted Rehabilitation Device for Post-Stroke

| | |
|---|---|
| $a$ | Link length |
| $\alpha$ | Link twist |
| $d$ | Link offset |
| $\theta$ | Joint angle |
| $T$ | Homogeneous transformation matrix |
| $s$ | Sine of the angle |
| $c$ | Cosine of the angle |
| $x_3$ | End-effector frame in x-direction |
| $y_3$ | End-effector frame in y-direction |
| $z_3$ | End-effector frame in z-direction |
| $x_0$ | Base frame in x-direction |
| $y_0$ | Base frame in y-direction |
| $z_0$ | Base frame in z-direction |
| $u_i$ | Tangent of any half angle |
| $q$ | Joint variables/3x1 vector of generalized joint coordinates |
| $v$ | Linear velocity |
| $\dot{q}$ | Angular velocity |
| $J$ | Jacobian |
| $J(q)$ | Jacobian matrix |
| $k$ | First derivative of the forward kinematics equation |
| $\tau$ | 3x1 vector of generalized input actuator forces/torque |
| $L$ | Lagrangian |
| $K$ | Kinematic energy of the robotic system |
| $P$ | Potential energy of the system |
| $M_r$ | Robot mass matrix |
| $I_{act}$ | Actuator inertia |
| $C(q, \dot{q})$ | Coriolis and centrifugal terms |
| $G(q)$ | Gravity term |

| | |
|---|---|
| $\tau_e$ | Vector of environment reaction torque |
| $f_e$ | Task space contact force |
| $M(q)$ | Sum of the total robot mass matrix and the actuators inertia |
| $M_m$ | Robot virtual impedance parameter of mass |
| $B_m$ | Robot virtual impedance parameter of damping |
| $K_m$ | Robot virtual impedance parameter of stiffness factors |
| $S$ | Selector matrix for force and position control |
| $f_d$ | Reference force |
| $x_d$ | Reference position |

## Wet Scrubber Design

| | |
|---|---|
| $\rho$ | Density |
| $A$ | Cross sectional area |
| $U_1$ | Inlet velocity |
| $U_2$ | Outlet velocity |
| $U_g$ | Maximum gas velocity |
| $m$ | Mass flow rate of the exhaust gas |
| $D$ | Cylindrical spay chamber diameter |
| $Z$ | Height of the scrubber system |
| $P_e$ | Collapsing pressure |
| $L$ | Length |
| $K_1$ | Numerical coefficients depending on the length to diameter ratio |
| $K_2$ | Numerical coefficients depending on the diameter to thickness ratio |
| $E$ | Modulus of elasticity |
| $t$ | Thickness |
| $Q$ | Quantity of liquid/discharge |
| $q$ | Quantity of discharge of each droplet |
| $v$ | Nozzle critical velocity |
| $a$ | Nozzle orifice |
| $N$ | Number of nozzles |
| $U_{crit}$ | Critical velocity |
| $d_{\sup}$ | Diameter of the supply pipe |
| $Q_{spray}$ | Quantity of liquid of the spray pipe |
| $d_{spray}$ | Diameter of the spray pipe |
| $d_{duct}$ | Duct diameter |
| $Q_{hf}$ | Volume of gas flowing through the frustum in one second |
| $H$ | Height of the hood |
| Re | Reynolds number |
| $h_D$ | Head loss due to friction in turbulent flow |
| $f$ | Darcy friction factor |
| $\varepsilon$ | Roughness of a pipe/turbulent kinetic energy dissipation rate |
| $k_C$ | Coefficient of contraction |

| | |
|---|---|
| $\theta$ | Cone angle |
| $k_{LN}$ | Frictional loss coefficient |
| $h_{TLN}$ | Total losses due to nozzles |
| $\Delta E$ | Rate of energy gain |
| $P_{pump}$ | Mechanical power delivered to the pump |
| $\eta_{pump}$ | Efficiency of the pump |
| $P_{electric}$ | Electric power of the motor |
| $\eta_{motor}$ | Efficiency of the electric motor |
| $E_{loss}$ | Lost mechanical energy |
| $\Delta T$ | Temperature rise |
| $\lambda$ | Scale factor |
| $\lambda_L$ | Length scale factor for the scrubber diameter, height and thickness |
| $\lambda_T$ | Time scale factor |
| $\lambda_U$ | Velocity scale factor |
| $\lambda_a$ | Acceleration scale factor |
| $\lambda_Q$ | Discharge scale factor |
| $\lambda_F$ | Force scale factor |
| $\lambda_\rho$ | Density scale factor |
| $T$ | Ratio of time |
| $T_p$ | Ratio of time required for homologous particles to travel in a prototype |
| $T_m$ | Ratio of time required for homologous particles to travel in a model |
| $a$ | Acceleration |
| $F_r$ | Scaled ratio of homologous forces |
| $F_m$ | Scaled ratio of homologous forces in the model |
| $F_p$ | Scaled ratio of homologous forces in the prototype |
| $EU$ | Euler number |
| $i$ | Direction vector |
| $j$ | Direction vector |
| $k$ | Turbulent kinetic energy |
| $\mu_t$ | Viscosity coefficient of turbulent flow |
| $\delta_k$ | Constant of 1.0 |
| $\delta_\varepsilon$ | Constant of 1.3 |
| $c_1$ | Constant of 1.44 |
| $c_2$ | Constant of 1.92 |
| $\phi_j$ | Concentration of chemical specie and $j$ is the particle matter particle size |
| $U_j$ | Particle matter velocity |
| $D_{diff}$ | Diffusivity of a scalar in the fluid |
| $F_g$ | Gravitational force |
| $F_D$ | Drag forces |
| $Stk$ | Particle stokes number |
| $\tau_j$ | Relaxation time |
| $\tau_f$ | Relevant fluid time scale |
| $\Delta P$ | Pressure drop |
| $P_{system}$ | System pressure |
| $P_{gauge}$ | Gauge pressure |

$P_{atm}$ Atmospheric pressure

## Development of Intelligent Controller for Pollution Monitoring and Control

$y_p(j, 0)$ Particulate matter concentration at the scrubber inlet
$Q_L/Q_G$ Liquid to gas ratio
$v_r$ Relative velocity between liquid droplets and dust particles
$v_g$ Gas velocity
$z$ Height of the scrubber
$d_D$ Droplet diameter
$\eta_{sep}$ Gas-particle separation efficiency
$\psi$ Impaction parameter
$C_{cf}$ Cunningham slip-correction factor
$\mu_g$ Gas viscosity
$v_{td}$ Terminal settling velocity of the liquid droplets
$\rho_p$ Particle density
$\rho_D$ Particle diameter
$\rho_g$ Gas density
$Kn$ Knudsen number
$\lambda$ Gas mean free path
$T_g$ Gas temperature
$P$ Atmospheric pressure
$M_g$ Molecular weight of the gas
$R$ Universal gas constant
$g$ Gravitational acceleration
$C_D$ Drag coefficient
Re Reynolds number
$v_{td}$ Terminal settling velocity
$N$ Number of membership functions for inputs and outputs
$M$ Number of membership functions for inputs and outputs
$L$ Number of membership functions for inputs and outputs
$V_{cal}$ Calculated voltage
$V_o$ Sensor analog voltage

## Optimal Tuning of Fractional-Order PID Controller for Electric Power-Assisted Steering (EPAS) System Using Particle Swarm Optimization (PSO)

$J_c$ Moment of inertia of the column

| | |
|---|---|
| $B_c$ | Column damping |
| $T_s$ | Torque sensor |
| $\theta_c$ | Rotation angle of the driving wheel |
| $T_d$ | Torque of driving wheel |
| $K_c$ | Steering column stiffness |
| $X_r$ | Rack horizontal displacement |
| $R_s$ | Radius of pinion steering |
| $T_m$ | Motor output |
| $J_m$ | Motor inertia |
| $B_m$ | Motor damping |
| $K_a$ | Motor torque |
| $R$ | Resistance |
| $L$ | Inductance |
| $K_b$ | Anti-EMF coefficient |
| $U$ | Motor voltage |
| $i_a$ | Motor current |
| $\theta_m$ | Angle of motor |
| $M_r$ | Steering tie rod mass |
| $B_r$ | Steering tie rod damping coefficient |
| $R_s$ | Radius of pinion steering |
| $K_r$ | Tire spring rate |
| $K(v)$ | Ratio coefficient |
| $I_{\max}$ | Maximum current |
| $C(S)$ | Transfer function of the controller |
| $K_p$ | Proportional gain |
| $K_i$ | Integral time constant |
| $K_d$ | Derivative time constant |
| $\lambda$ | Fractional power |
| $\mu$ | Fractional power |
| $v_i$ | Velocity of particle i |
| $w$ | Inertia weight factor |
| $x_i$ | Particle position |
| $rand$ | Random function |
| $C_1$ | Acceleration constant |
| $C_2$ | Acceleration constant |
| $P_{best}$ | Best position of the i$^{th}$ particle |
| $G_{best}$ | Best position among all particles in the swarm |
| $W$ | Weight function |
| $W_{\max}$ | Initial weight |
| $W_{\min}$ | Final weight |
| $iter$ | Current iteration time |
| $iter_{\max}$ | Maximum number of iterations |
| $T_s$ | Setting time |
| $T_r$ | Rise time |
| $M_p$ | Overshoot |

| | |
|---|---|
| $e_{ss}$ | Steady-state error |
| $ISE$ | Integral of squared-error |
| $ITSE$ | Time-weighted-squared-error |
| $IAE$ | Integrated absolute error |
| $a$ | Weighting factor |

## Forward Navigation for Autonomous Unmanned Vehicle in Inter-Row Planted Agriculture Field

| | |
|---|---|
| $B_i$ | Bernstein function |
| $CP_n$ | Control vector |
| $x$ | Point at x-plane |
| $y$ | Point at y-plane |
| $H$ | Distance |
| $V$ | Velocity |
| $\delta t$ | Total elapsed time |

## Hardware Design and Development of Contactless Sensor System for Piano Playing

| | |
|---|---|
| $C$ | Capacitance |
| $\varepsilon$ | Dielectric constant of the material between the two conducting plates |
| $A$ | Area of both conducting plates |
| $d$ | Distance between two conducting plates |

## The Validation of Virtual Impact Tests Using LabVIEW Instrumentation Techniques

| | |
|---|---|
| $P(t)$ | Impact force respect to time |
| $P_{\max}$ | Maximum force |
| $R$ | Radii curvature |
| $t$ | Time after the impaction |
| $\tau_c$ | Contact period |
| $K$ | Constant regarding the material and dimension properties of the surfaces |
| $V_1$ | Initial impact velocity of the hammer |
| $e$ | Coefficient of restitution |
| $m_1$ | Mass of the hammer |
| $v_1$ | Poisson's ratio of the hammer surface |

| | |
|---|---|
| $v_2$ | Poisson's ratio of the plate surface |
| $E*$ | Relative elastic moduli of the contacting surfaces |
| $E_1$ | Elastic moduli of the hammer surface |
| $E_2$ | Elastic moduli of the plate surface |
| $w(x, y)$ | Transverse displacement of the plate |
| $q(t)$ | Temporal equation that deals with frequency of the natural vibration |
| $x$ | Impacted point X |
| $y$ | Impacted point Y |

## Instrumentation in Underwater Environment

| | |
|---|---|
| $SPL$ | Sound pressure level |
| $SL$ | Source level |
| $N$ | Transmission loss |
| $R$ | Distance from the source |
| $a$ | Coefficient of absorption |

## BER Performance Evaluation of M-PSK and M-QAM Schemes in AWGN, Rayleigh and Rician Fading Channels

| | |
|---|---|
| $Q$ | Q-function |
| $K$ | Rician factor |
| $Eb$ | Ratio of energy per bit |
| $No$ | Spectral noise density |
| $P$ | Equation of bit error rate for binary phase-shift keying |
| $N$ | Rician fading channel diversity |
| $M$ | M value of M-ary Quadrature Amplitude Modulation (M-QAM) modulation scheme in additive white Gaussian Noise |

## Camera Calibration and Video Stabilization Framework for Robot Localization

| | |
|---|---|
| $f$ | Focal length |
| $b$ | Baseline |
| $z$ | Distance computed |
| $\varepsilon$ | Error |

# Introduction

**Rini Akmeliawati**

**Abstract** The series of research collections, CONTROL ENGINEERING IN ROBOTICS AND INDUSTRIAL AUTOMATION, presents research outcomes in the fields of, but not limited to, control engineering, mechatronics, robotics and automation. The book's eleven chapters demonstrate the current state-of-the-art technology in the aforementioned fields. Research work on a rehabilitation robotic device, web-scrubber systems, swarm robots, an electric power-assisted steering system (EPAS), a navigation system for an unmanned vehicle as part of agricultural technology, a sensor-based piano-playing analyzer, a steel-plate virtual impact tester, a review work on underwater instrumentations, an efficient wireless communication system for sensor data and vision-based robot localization are presented in this book. These diverse contribution will be beneficial to researchers, industrialists and whoever else is interested in the topics.

Control technology is an engineering field that involves multiple disciplines in its development and applications; however, it is often 'hidden' within various other branches of technology. It is in fact a branch of the engineering field that becomes a key enabler to several technological applications and is considered the 'brain' of any mechatronics systems. Control technology often comes together with sensor and measurement technology, as we will see in this volume.

In this first series of research collections, various applications of control engineering, sensors, and instrumentation technology in robotics and industrial automation, and other mechatronics, navigation and communication systems, are presented.

Control applications for an end-effector robotic device for upper-extremity rehabilitation is presented by Sidek and Fatai. Such a robotic device is aimed to help hemiparetic post-stroke patients. It offers three-degrees-of-freedom motions for elbow and shoulder exercise. The controller is designed based on an adaptive hybrid impedance

R. Akmeliawati (✉)
School of Mechanical Engineering, The University of Adelaide, Adelaide, SA 5005, Australia
e-mail: rini.akmeliawati@adelaide.edu.au

 
M. Mariappan et al. (eds.), *Control Engineering in Robotics and Industrial Automation*, Studies in Systems, Decision and Control 371,
https://doi.org/10.1007/978-3-030-74540-0_1

framework for safe robot–patient dynamic interactions during repetitive exercises and monitors the patients' motor recovery.

An intelligent control system finds an interesting application in web scrubber systems, as presented by Umar and Salami. The controller is used to adjust the flow rate of the liquid pump to deliver the appropriate droplet size for scrubbing the Particulate Matter (PM) contaminants based on their detected concentration level. As a result of the implementation of the designed intelligent controller, the web scrubber system can maintain the emission size below the recommended value in less than 10seconds. The details of the designed web scrubber system is provided in the preceding chapter by Danzomo et al.

Majid et al. present an interesting technical review on swarm robotics' behaviors and tasks. The review provides an overall overview of research in swarm robotics tasks, which are classified into two types: low-level and high-level tasks. The chapter identifies and shows the correlation between the two types of tasks. The review also includes the software and hardware platforms used for simulation and experimentation in swarm robotics research.

Still related to swarm behaviors, Hassan et al. show the application of a particle swarm optimization algorithm as a tuning mechanism for Fractional-Order PID (FOPID) controllers for the electric motor of an Electric Power-Assisted Steering system (EPAS). The performance of the overall system is evaluated under different speeds and driver torques. The optimal FOPID with PSO has demonstrated a more efficient performance than a classical PID controller to the system.

An autonomous navigation system of a small-scaled unmanned vehicle for agriculture applications has been proposed by Thamrin et al. Forward and headland turn navigation based on the Bezier curve provides optimized trajectory planning for the autonomous vehicle to perform narrow inter-tree navigation in an agricultural field. This is essential for precision agriculture systems.

The application of sensor technology is not only limited to the engineering field but can also be found in music. Choo and Mariappan propose the design of a contactless sensor system to study the finger positions of musicians while playing the piano. A non-intrusive and long-range capacitive sensor is developed and placed under the keyboard area to sense the position of the player's fingers on five piano keys. An artificial neural network is used to process the data such that the pianists can store and analyze their playing techniques.

The application of sensor and instrumentation technology is also found in impact testing, as described by Chong et al., who propose the LabVIEW-based instrumentation to validate virtual impact tests of steel plates with various boundary conditions. The piezoelectric accelerometer is used as the primary sensor in the instrumentation, providing excellent means of dynamics measurements of the impact incidents. The LabVIEW-based instrumentation was used for hammer drop tests to investigate the impact response of the steel plate with different hammer heights and various boundary conditions.

Rashid and Ahmad present a review on state-of-the-art underwater instrumentation to measure environmental underwater noise. Underwater measurements are affected by various parameters, such as distance, fish population, sound, and other uncertainties due to oceanic activities. Advances in sensors and measurement techniques are improving the accuracy and quality of the measurement data under such conditions. The review describes the construction, operation and performance of various underwater instrumentation and measurement techniques for specific applications, such as noise, sound, distance and direction measurements, fish population estimation, and mine detection.

Controllers and their sensors are linked through communication systems. Efficient wireless communication systems are essential in transmitting information, such as sensor data. Minimum errors can be achieved with proper channel conditions and modulation techniques. Farzamnia et al. investigate and compare the Bit Error Rate (BER) performance of two modulation techniques which are used in communications systems, the M-ary Phase Shift Keying (M-PSK) and M-ary Quadrature Amplitude Modulation (M-QAM), under the Additive White Gaussian Noise (AWGN), Rayleigh and Rician fading channels.

Another application of control and sensor technology can be found in robot localization problems. In the last chapter of this volume, Sahran et al. investigate two major issues in vision-based localization: camera calibration and video stabilization. A stereo-vision method using Fuzzy Camera Calibration (FCC), Fuzzy Optical Flow (FOF) and Fuzzy Gaussian Pyramid methods is proposed to improve robot localization.

As described, 11 chapters which focus on control and sensor technology and their related systems are included in this volume. We hope that the contributions can enlighten the readers with various applications of control and sensor technology and the cutting-edge research in this field. The chapters will be beneficial to researchers, graduates, academics, and industrialists who have interests in and/or are dealing with such technology, whether directly or indirectly.

# Design and Control of a 3D Robot-Assisted Rehabilitation Device for Post-Stroke

**Shahrul Na'im Sidek and Sado Fatai**

**Abstract** With the ever-increasing population of stroke patients requiring rehabilitation therapy compared with the few available therapists, what is now crucial is an adaptive system that can complement closely the role of an expert therapist by sensing the patients' muscle tone, physical recovery condition, or sensorimotor control performance to specify appropriate therapy and to provide an assessment. A "high-level" adaptive hybrid impedance controller based on Modified Ashworth Scale (MAS) assessment criteria for rehabilitation of the upper extremity of post-stroke patients was therefore proposed and discussed in this chapter. An end-effector-based 3 degree-of-freedom (3-DOF) rehabilitation platform was developed with the proposed control strategy with the emphasis on proper joint coordination and control to actualize effective trajectory tracking and consequently effective therapy.

## 1 Introduction

Rehabilitation therapy post-stroke is crucial in helping patients to regain as much possible use of their paretic limbs in the activities of daily living. The major challenge, however, in contemporary post-stroke rehabilitation therapy especially in the post-acute phase of stroke recovery is that the therapy is time-demanding and labor-intensive. Therefore, expensive with a consequent reduction in the amount of training sessions required for optimal therapeutic outcome. In recent years, the use of robotic devices for rehabilitation therapy has been widely favored. Robot-assisted rehabilitation therapy is cost-effective, fatigue-free, and has the potential to improve the efficiency of the rehabilitation process. More so, positive outcomes of improved motor control abilities for patients undergoing robot-assisted therapy have been widely recorded through proper developed exercise programs that are usually task-specific and intensive, and require progression of difficulty.

S. N. Sidek (✉) · S. Fatai
Department of Mechatronics Engineering, International Islamic University Malaysia, P.O. Box 10, 50728 Kuala Lumpur, Malaysia
e-mail: snaim@iium.edu.my



M. Mariappan et al. (eds.), *Control Engineering in Robotics and Industrial Automation*, Studies in Systems, Decision and Control 371,
https://doi.org/10.1007/978-3-030-74540-0_2

This chapter presents the development and control of a portable 3-DOF end-effector-type robotic device for upper-extremity rehabilitation for hemi-paretic post-stroke patients. The device has three active DOFs consisting of two revolute joints and one prismatic joint (R-R-P) designed to allow three-dimensional range of motion (ROM) exercise for elbow and shoulder rehabilitation. An adaptive hybrid impedance control framework has also been developed for the device to allow safe robot–patient dynamic interaction during the planned repetitive range of motion exercises and to keep track of patients' motor recovery based on an embedded Modified Ashworth Scale (MAS) muscle assessment criteria. Experimental results performed, using a healthy subject, to test and evaluate the ability of the device to track a planned simple flexion/extension range of motion exercise for the elbow joint showed the possibility of use of the device for real patients.

## 2 Background

In the last few decades, the increasing cases of upper-extremity disabilities resulting from stroke, spinal cord injuries (SCI), and other related illness have favored the use of robotic devices to provide assistance and support to patients undergoing rehabilitation therapy [11, 14]. The effectiveness of the devices in extending the therapy session and in providing repetitive exercises aimed at inducing motor plasticity have been widely reported [8, 11]. Robotic devices have the potentials of allowing repeatability and automation of therapeutic procedures with significant improvement on the efficiency of the rehabilitation process [13]. With the increasing demand, for robotic devices, the need for portable, lightweight, and safety devices have created new challenges ranging from the design of compact robot mechanical/actuation systems to the development of effective control algorithms.

A survey on robotic devices in the recent past showed that most of the earlier robotic devices and some of the recent commercially available ones are mechanically bulky and suited for use only in rehabilitation centers [2, 4, 5]. Besides, most are less autonomous to the extent that they require constant assistance of a human therapist for effective usage, for task specification, and for difficulty level adjustment of therapy [5]. This implies a considerable amount of valuable therapist time in programming the robot, monitoring the patients, analyzing data from the robot, and also assessing the progress of the patients. Krebs et al. [6, 10] earlier proposed a 3-DOF robotic device that allowed the horizontal motion and a 6-DOF Mirror Image Movement Enabler (MIME) robotic device that allowed three-dimensional spatial motion respectively for upper-limb rehabilitation which was generally bulky and suited only for rehabilitation centers. The devices were less autonomous and require the manual monitoring of patients' progress by an expert therapist. A 9-DOF cable-driven robotic device was also proposed by Loureiro et al. [9] based on GENTLE/S system. The device was effectively used for reach and grasp therapy for post-stroke patients but was equally bulky and non-adaptive to patients' recovery. A more recent commercially available robotic device referred to as Armeo Power [12] with 7-DOF for elbow and shoulder rehabilitation and additional DOFs for wrist and fingers flexion/extension rehabilitation exercise which has been successfully used in many rehabilitation centers is also seen to be largely stationary and not lightweight. As the development of robotic devices for rehabilitation exercises continues, the need for portable and lightweight devices capable of autonomous guidance and monitoring of patients' progress, therefore, remains a critical driving factor of consideration [5].

In this chapter, the development and control of a 3-DOF end-effector robotic device for autonomous rehabilitation of the shoulder and elbow region of patients with hemi-paretic upper-limb impairment is presented. The device is made portable and lightweight to allow flexibility of usage and for possible use at homes. In addition, a novel adaptive control framework as reported in Sado et al. [15] is developed for the device to allow safe robot–patients dynamic interaction and effective tracking of a planned range of motion exercise, and independent monitoring of patients' physical recovery progress.

## 3 System Description

### *3.1 System Modeling—Forward Kinematics*

The robotic device has three active DOFs arranged in a revolute–revolute–prismatic (R–R–P) configuration as shown in Fig. 1. The three joints allow for the rehabilitation (flexion, extension, abduction, and adduction) of the elbow and shoulder of the patients in three-dimensional space. The relationship between the joints variables and the position and orientation of the robot's end-effector is derived from the four Denavit–Hartenberg (DH) parameters given in Table 1. The four parameters $a_i$, $\alpha_i$, $d_i$, $\theta_i$ are generally known as the link length, link twist, link offset, and joint angles respectively [16].

The link transformation matrices which relate any two successive frames attached to the joints are derived from the homogenous transformation matrix [16] given by Eq. (1).

$$ {}^{i-1}_{i}T = \begin{bmatrix} c\theta_i & -s\theta_i & 0 & a_{i-1} \\ s\theta_i c\alpha_{i-1} & c\theta_i c\alpha_{i-1} & -s\alpha_{i-1} & -s\alpha_{i-1} d_i \\ s\theta_i s\alpha_{i-1} & c\theta_i s\alpha_{i-1} & c\alpha_{i-1} & c\alpha_{i-1} d_i \\ 0 & 0 & 0 & 1 \end{bmatrix} \tag{1} $$

where $s$ and $c$ stands for sine and cosine of the angles. The homogenous transformation matrix relating the end-effector frame ($x_3$, $y_3$, $z_3$) to the base frame ($x_0$, $y_0$, $z_0$), see Fig. 1, is therefore obtained by multiplying the individual link transformation matrices as shown in Eq. (2).

$$ {}^{0}_{3}T = {}^{0}_{1}T \times {}^{1}_{2}T \times {}^{2}_{3}T \tag{2} $$

Fig. 1 The robot kinematic model

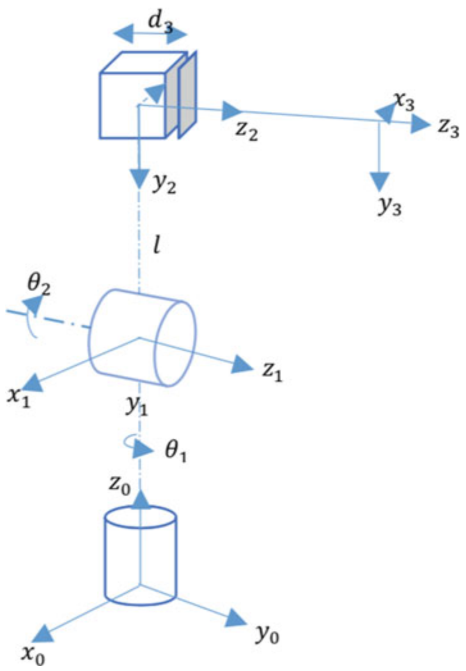


**Table 1** The DH-parameters

| Link | $a_i$ | $\alpha_i$ | $d_i$ | $\theta_i$ |
|---|---|---|---|---|
| 1 | 0 | −90 | 0 | $\theta_1$ |
| 2 | 1 | 90 | 0 | $\theta_2$ |
| 3 | 0 | 0 | $d_3$ | 0 |

Finally, the forward kinematics equation derived from Eq. (2) is expressed as Eq. (3).

$$\begin{bmatrix} x \\ y \\ z \end{bmatrix} = \begin{bmatrix} c\theta_1(lc\theta_2 + d_3 s\theta_2) \\ s\theta_1(lc\theta_2 + d_3 s\theta_2) \\ d_3 c\theta_2 - ls\theta_2 \end{bmatrix} \tag{3}$$

## 3.2 System Modeling—Inverse Kinematics

The inverse kinematics of the rehabilitation robot is derived in order to determine the joint angles or variables in terms of the end-effector position and orientation. It is however more computationally demanding than the forward kinematics analysis due to the non-linearity in the forward kinematics equation. Since the robotic device is designed with two-axis intersecting, the inverse kinematic analysis becomes fairly easy with a possible closed-form solution.

Observing that the forward kinematics equations are transcendental, the following substitutions are made:

$$u_i = \tan\frac{\theta_i}{2}\ ,\ \cos\theta_i = \tfrac{1-u_i^2}{1+u_i^2}\ ,\ \sin\theta_i = \tfrac{2u_i}{1+u_i^2} \tag{4}$$

where $u_i$ denotes the tangent of any half angle, and $i = 1, 2$. By substituting Eq. (4) in Eq. (3) and solving for the joint variables $q = [\theta_1\ \theta_2\ d_3]$, the inverse kinematics equations for the robotic system is obtained as follows:

$$\left.\begin{array}{c} \theta_1 = A\tan2(\pm\frac{y}{x}, 1) \\ \theta_2 = A\tan2(-l \pm \sqrt{l^2 + \left(\frac{d_3-z}{d_3+z}\right)}, 1) \\ d_3 = \pm\sqrt{x^2 + y^2 + z^2 - l^2} \end{array}\right\} \tag{5}$$

The solution is however not unique since there is the possibility of different configurations (some unreachable) for a given solution. Therefore, the use of inverse kinematics for controller development is avoided as will be seen in the next section.

### 3.3 System Modeling—Velocity Kinematics: The Jacobian

The velocity kinematics equation relates the linear velocity, $v$ and angular velocity, $q$ of the end-effector to the joint velocities of the robotic device. Similar to the forward kinematics equation, it defines the map between the Cartesian space and joint space. This relationship is expressed by the Jacobian time-varying linear transformation given by Eq. (6).

$$v = J(q)\dot{q} \tag{6}$$

Taking the first derivative of the forward kinematics equations (refer to Eq. 3) and using the techniques described in Spong et al. [16], the Jacobian, $J$ is obtained and given as

$$J = \begin{bmatrix} -s_1(lc_2 + d_3 s_2) & -c_1(lc_2 + d_3 s_2) & c_1 s_2 \\ c_1(lc_2 + d_3 s_2) & -s_1(lc_2 + d_3 s_2) & s_1 s_2 \\ 0 & k & c_2 \\ 0 & -s_1 & 0 \\ 0 & -c_1 & 0 \\ 1 & 0 & 0 \end{bmatrix} \quad (7)$$

where $k =- c_1^2(lc_2 + d_3 s_2) - s_1^2(lc_2 + d_3 s_2)$

### *3.4 System Modeling—the Robot Dynamics*

To obtain the robot dynamic model, the Lagrange equation of motion for a conservative system is adopted and given by Eq. (8)

$$\frac{d}{dt}\frac{\partial L}{\partial \dot{q}} - \frac{\partial L}{\partial q} = \tau \quad (8)$$

where $q$ is the $3 \times 1$ vector of generalized joint coordinates, $\tau$ is the $3 \times 1$ vector of generalized input actuator forces/torque, and $L$ the Lagrangian.

The Lagrangian is given by the expression

$$L = K - P \quad (9)$$

where $K$ is the kinematic energy of the robotic system and $P$ is the potential energy of the system. Using Eqs. (8) and (9), the overall dynamic model of the robotic device is derived and expressed by Eq. (10) which is a requisite for developing the control algorithm.

$$M_r(q)\ddot{q} + I_{\mathrm{act}}\ddot{q} + C(q, \dot{q})\dot{q} + G(q) = \tau \quad (10)$$

$M_r$ represents the robot mass matrix, $I_{act}$ represents the actuator inertia, $C(q, \dot{q})$ represents the Coriolis and centrifugal terms, and $G(q)$ represents the gravity term. Since the joint frictions are small for the robotic device, these components are assumed negligible in the robot dynamic model.

### *3.5 Control Architecture—Sensors and Actuation System*

A DC motor coupled at the prismatic joint, at frame $(x_2, y_2, z_2)$, provide linear actuation by means of a lead screw mechanism to allow flexion and extension of the